Evolution of water waves generated by subaerial solid landslide

S. Viroulet[1,*], D. Cébron[2], O. Kimmoun[1], and C. Kharif[1]

[1]Aix-Marseille Univ., IRPHE (UMR 6594), 13384, Marseille cedex 13, France.
[2]Inst. für Geophysik, Sonneggstrasse 5, ETH Zürich, Zürich, CH-8092, Switzerland.
[*]viroulet@irphe.univ-mrs.fr

Abstract

Waves generated by aerial and subaerial landslides are studied experimentally, theoretically and numerically. A set of experiments are done in a wave tank of 18 m long, 0.65 m wide and 1.5 m deep. Numerical simulations are in good agreement with the experiments. Based on numerical and experimental results, we derive different scaling laws which show a good agreement with the experiments and the simulations. These scaling laws allow thus to predict the time evolution of the maximum amplitude wave generated by an aerial solid landslide, which is a relevant quantity for wave forecast.

1 Introduction

The modelisation of landslide tsunamis are more difficult than those generated by tectonic source due to the lack of knowledge of the mechanism and interactions between water and slide. Previous works have been realized on submarine and aerial landslides trying to better understand the influence of the slide parameters on the generated waves. Experimentals investigations have been done using solid body [12, 8] or granular materials [4, 2]. They show that the most important parameters are the size and rigidity of the slide, the impact velocity and the initial submergence. Several methods were used to reproduce water waves generated by landslides. From nonlinear shallow water equations [7] to potential flow [6] or Smoothed Particles Hydrodynamics [9]. More recently, Abadie [1] used a multiple-fluid Navier-Stokes model using a VOF method to track the interface and the interactions between slide/air/water. To study the influence of the main parameters of a solid landslide generating waves, we performed severals experiments in a wave tank with a solid body sliding down an incline plane. The initial mass and position of the solid are changed to create subaerial and aerial landslides. Based on initial numerical results, we performed additionnal numerical experiments, we systematicaly study the influence of the slide velocity, the slope inclinaison, the initial water depth and the shape of the solid on the generated water waves in near and far field. The main objectives of this work are to validate the accuracy of the code in the prediction of free surface elevation and develop a parametric model of prediction of wave generation and propagation as a function of the initials configurations of an aerial solid landslide.

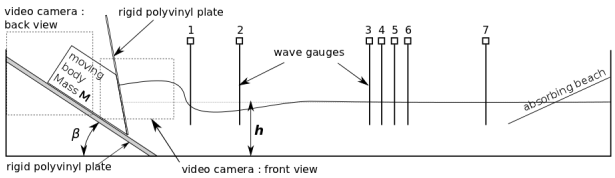

Figure 1: *Schematic of the experimental set up for subaerial landslide generated waves.*

2 Experimental set-up and data acquisition

Experiments are performed at École Centrale de Marseille in a 18 m long, 0.65 m wide wave tank. A plane slope was installed at one side of the flume and an absorbing beach at the other. The slope consist of a polyvinyl plane fixed to the left boundary with 35° inclinaison. The water depth was about 0.43 m and 0.38 m (see fig.1). The solid used to generate the impulse wave was represented by a box with a front angle of 45°. The wedge slides down the slope by gravity rolling on four wheels. The sides of the tank are made of transparent glass. We have used two cameras to follow the displacement of the solid and the evolution of the free surface in the generation zone. To track the propagation and measure the amplitude of the generated waves, seven wave gauges are installed along the wave tank at respectively 1.80 m, 2.805 m, 4.98 m, 5.16 m, 5.34 m, 5.70 m and 10.08 m from the intersection of the slope with the bottom of the flume. Several experiments are performed changing the water depth, the mass and the initial position of the solid. A high position where the front of the mobile was located 3 cm

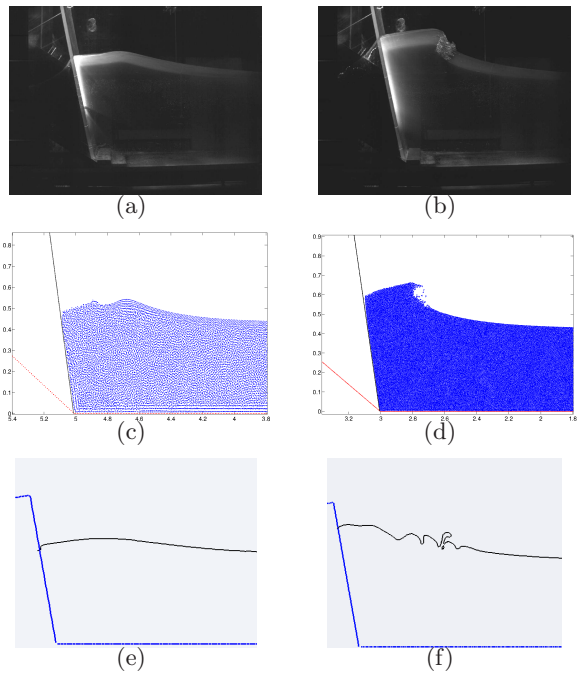

Figure 2: *Comparison between the experiment and the simulated free surface for both initial configurations : left side, low position, right side high position when the solid reach the bottom of the tank.*

below the free surface and a low one located 25 cm underwater.

3 Experimental and numerical results

Two different models are used to simulate landslide tsunami in the set-up discribed previously. Gerris an open source tree-based adaptative solver using finite-volume discretisation and adaptative mesh refinement to solve Navier-Stokes equation [11] and SPHYSICS[2], which derives from an existing open-source 2D SPH code [3, 5]. Simulations with Gerris are done in a 12 m × 12 m square domaine, the edge of our smaller cell is about 6 mm. We keep the real value of density and viscosity. SPHYSICS[2] simulate monophasic flows with a free-surface and moving solids in the numerical 5 m long domain. The influence of the air flows is neglected on these simulations, which can lead to slitghly enhanced wave height. The velocity of the solid is directly imposed, in the numerical simulations, from the experimental records of its displacement along the incline. A comparison between a snapshot of the free surface elevation and modelized wave profiles for both configuration are shown in figure 2. In both cases, SPH results are in a better agreement, especially for the higher configuration, where the wave braking is clearly modelized (three times more particles are used for this simulation). With Gerris this phenomena is not well modelized (even with higher resolution), os-

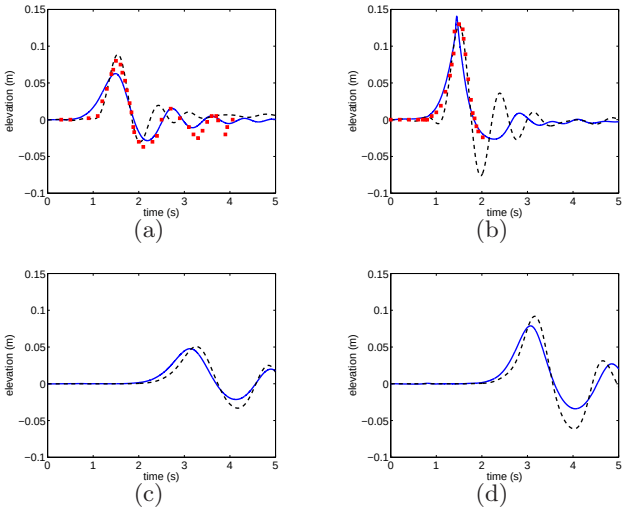

Figure 3: *Wave gauges at* 1.80 *m (a,b) and* 5.16 *m (c,d). Comparison between experimental and computed waves (a,c) low position, (b,d) high position. Dashed black line represent the experiment, blue continuous line Gerris and red squares SPH simulation.*

cillations on the free surface are assume to be a kind of wave breaking. For the lower case, the amplitude seem under-estimated.

Comparison between experimental and numerical wave gauges 1 and 4 for low and high configuration is shown in figure 3(a,c) and (b,d) respectively. The amplitude of the first crest is well captured with SPH whereas Gerris underestimate it for the lower position. Both codes are in satisfactory agreement for the amplitude of the trough following the first crest and the dispersive tail for the lower configuration. In the higher case, Gerris and SPH results are also in excellent agreement with the experiments for the amplitude of the first crest, but the following trough and second crest are drastically underestimated. At the fourth probe, located at 5.16 m (out from the SPH domain) the amplitude of the first crest and the following dispersive tail are in good agreement with the experiments in both configurations. Both models reproduce well the generation and the propagation of waves generated by subaerials landslides. Whereas SPH is more accurate in the generation zone, it required a longer CPU time than Gerris. However, despite the lower accuracy in the initial formation of the wave, Gerris reproduces well the overall behavior during the propagation, together with a shorter computation time.

4 Scaling law

To predict the main characteristics of water waves generated by aerials solid landslides, especially the evolution and the travel time of the maximum amplitude, we consider the relevant parameters of the experiments : the velocity of the solid, V, the water depth, H, the

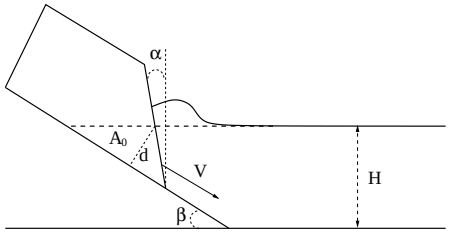

Figure 4: *Schematic of the numerical experiments with the representation of α, β, H, the area of the submerged part of the solid A_0 and the thickness of the slide d.*

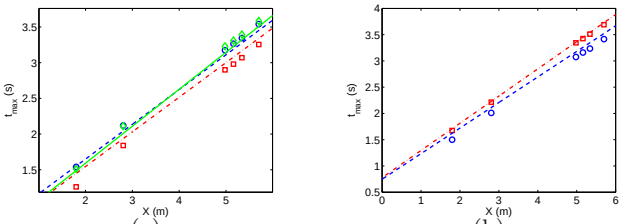

Figure 5: *Comparison between experimental and theoretical arrival time for the maximum amplitude. (a) low positions, dashed blue line and blue circles represent the theory and the experimental wave gauge for a water depth $H = 0.43$ m and a solid mass of 70 kg. The experiment represented by red squares and the theory by dash dotted red line, for a mass of 85.5 kg. Continuous green line and green diamonds represent the theory and the experimental results for a water depth $H = 0.38$ m and a solid mass of 85.5 kg. (b) high position : dashed blue line and blue circles represent the theory and the experimental wave gauge for a water depth $H = 0.43$ m and a solid mass of 85.5 kg. Continuous red line and red squares represent the same experiment with a lower water depth $H = 0.38$ m.*

slope angle β, the angle between the front of the solid and the vertical α and the gravity g. It consist of an aerial solid landslide where the mobile initially reachs the undisturbed free surface. The dimensional analysis is made in shallow water approximation $kh \ll 1$, and generated waves are supposed to be linear, $A/H \ll 1$. We want to extend these hypotheses to weakly dispersive nonlinear waves.

4.1 Arrival time

Contrary to earthquake tsunami, where the seafloor deformation occurs instantaneously in comparison of the wave speed and thus do not influence the propagation, waves generated by aerials and submarine landslides need an additional term in the equation of propagation. This term is represented by the travel time of the landslide. The arrival time of the maximum amplitude wave generated by aerial landslides can be interpreted as the moving time of the slide down along the incline added to the travel time of a linear solitary wave in water depth H.

$$t_{max} = \frac{H}{V \sin\beta} + \frac{X}{\sqrt{gH}}. \qquad (1)$$

with X the distance from the source. Figure 5 represents the comparison between the experimental arrival time for the maximum amplitude and the theory. Figure 5.(a) and (b) shows results for low and high positions, respectively. The maximum amplitude arrival time does not vary a lot. Dispite this the theory is in very good agreement with the experiments, the trend is good with the arrival time increasing for the last probes when the water depth is lower. The theory is in excellent agreement with the experiments.

4.2 Prediction of the amplitude evolution

In weakly nonlinear shallow water approximation, the amplitude evolution of an initial perturbation can be modelized by the linearized non-viscous Korteweg-de-Vries equation :

$$\frac{\partial \eta}{\partial t} + c\frac{\partial \eta}{\partial x} + \frac{c\,h^2}{6}\frac{\partial \eta^3}{\partial x^3} = 0. \qquad (2)$$

with η the free surface elevation and c the celerity of the wave. A solution of equation (2) is the following Green function [10], based on a Airy function:

$$\eta(x,t) = Q\left(\frac{2}{c\,t\,h^2}\right)^{1/3} \mathrm{Ai}\left[\left(\frac{2}{c\,t\,h^2}\right)^{1/3}(x - c\,t)\right]. \qquad (3)$$

This solution represents a leading long wave followed by a modulated wave train. This can be compared to our problem where an initial perturbation is produced by the landslide then propagates and disperses. With $c = \sqrt{gH}$ and Q, a typical area of the perturbation problem. Depending on the value of the Froude number, this area can be defined in two ways. We assume that all the energy of the slide is transfered in the generated wave. For strong impact where $Fr > 0.5$ we assume that the area of the perturbation is the same as the under water part of the slide A_0. For slower cases $Fr < 0.5$ we assume that the aera is equal to the thickness of the slide $d = (H\cos(\alpha+\beta))/\cos\alpha$ multiply by a typical length of the problem. These hypothesis lead to the following equations : For $Fr < 0.5$:

$$\eta_1 \sim K_4\,\kappa\,\frac{2^{1/3}\cos(\alpha+\beta)}{\cos\alpha}\,A_0^{1/4}\,V\,H^{1/6}g^{-2/3}\sqrt{\frac{t}{t_{solid}}}$$

$$\eta_2 \sim K_4\,\kappa\,\frac{2^{1/3}\cos(\alpha+\beta)}{\cos\alpha}\,A_0^{1/4}\,V\,H^{1/6}g^{-2/3}$$

$$\eta_3 \sim K_2\,\kappa\,\frac{2^{1/3}\cos(\alpha+\beta)}{\cos\alpha}\,A_0^{1/4}\,V\,H^{1/6}g^{-2/3}\,t^{-1/3}$$

For $Fr > 0.5$:

$$\eta_1 \sim K_3\,\kappa\,2^{1/3}\,A_0\,H^{-5/6}g^{-1/6}\sqrt{\frac{t}{t_{solid}}}$$

$$\eta_2 \sim K_3\,\kappa\,2^{1/3}\,A_0\,H^{-5/6}g^{-1/6}$$
$$\eta_3 \sim K_1\,\kappa\,2^{1/3}\,A_0\,H^{-5/6}g^{-1/6}\,t^{-1/3}$$

With :

$$A_0 = \frac{H^2\cos(\alpha+\beta)}{2\,\sin\beta\,\cos\alpha}. \quad (4)$$

The area of the submerged part of the slide. K_i $(i = 1, 4)$ are adjustable prefactors and κ the maximum value of the Airy function. Where η_1 represents the evolution when the solid is in movement. To fit to the second asymptotic solution η_2, which represents the transition zone between both asymptotic solutions, we divide the time dependence of η_1 by t_{solid}. The third solution, η_3, represents the propagation of the generated wave.

4.3 Comparison with our experiments

Several assumptions are made to compare the theory and the experiments, for instance on the velocity of the body (which is not constant here). For the propagation zone a relevant value is the mean velocity of the solid along its displacement. For the generation we take the velocity of the experiment. Figure 6 shows comparison between experimental, numerical and theoretical amplitude evolution as a function of time for two subaerial experiments. For each experiment only the water depth is changed, $H = 0.43$ m and $H = 0.38$ m on figure 6(a) and (b), respectively. The amplitude obtained by SPH is a slightly higher than Gerris, however the overall behavior remains the same. Because of the vicinity to our model limit ($Fr = 0.48$), both theories are represented in the propagation zone, as expected, experimental results are located between them. In the generation zone, the theory underestimates the numerical results but the overall behavior is well captured. For the lower water depth, the Froude number is about 0.42, only one theory is represented in the propagation zone. In the generation zone, the theory, numerical and experimental results are in an excellent agreement.

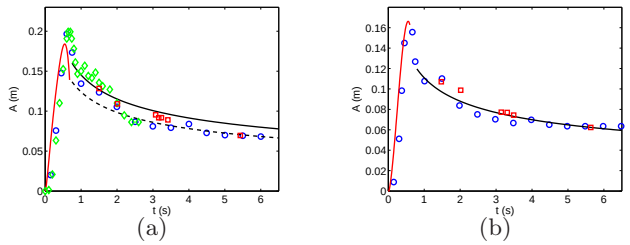

Figure 6: *Evolution of the amplitude as a function of time, (a) $H = 0.43$ m, (b) $H = 0.38$ m. Red squares represents, the experiment (the six wave gauges), blue circles Gerris simulation, green diamonds SPH simulation, red continuous line theory with $Fr > 0.5$, dashed and continuous black lines represents the theory in the propagation zone for $Fr > 0.5$ and $Fr < 0.5$ respectively.*

5 Conclusion

Experiments of solid landlside generated impulse waves were performed and numerically simulated using two methods. Numerical results was then used to obtained a scaling law on the amplitude and the propagation of the generated waves. This work, we can said that Gerris and SPHYSICS[2] can reasonably well modelized tsunami generated by aerial and subaerial solid landslides. Scaling laws are in agreement with experiments to predict the amplitude evolution as a function of time. Further experimental and numerical simulations of aerial landslides with granular material are under study. We aim to adapt the theory, especially in the generation, with a deformable aerial landslide which represents more realistic events.

References

[1] S. Abadie, D. Morichon, S. Grilli, and S. Glockner. *Coastal Eng.*, 57(9):779–794, 2010.

[2] B. Ataie-Ashtiani and A. Nik-Khah. *Environmental Fluid Mechanics*, 8(3):263–280, 2008.

[3] D. Cébron and J.F. Sigrist. *Proceedings of the 8th Int. Conf. on Hydrodynamics*, pages Nantes, France, 2008.

[4] H.M. Fritz. PhD thesis, Swiss Federal Institute of Technology Zürich, 2002.

[5] M. Gómez-Gesteira, B.D. Rogers, R.A. Dalrymple, A.J.C. Crespo, and M. Narayanaswamy. 2010.

[6] ST Grilli, P. Watts, and F. Dias. *Euro. Geophys. Soc. 26th General Assembly, Nice, France*, 2001.

[7] P. Heinrich, A. Piatanesi, and H. Hebert. *Geoph. J. Int.*, 145(1):97–111, 2001.

[8] P.L.F. Liu, T.R. Wu, F. Raichlen, C.E. Synolakis, and J.C. Borrero. *J. Fluid Mech.*, 536(1):107–144, 2005.

[9] JJ Monaghan and A. Kos. *Phys. Fluids*, 12:622, 2000.

[10] E. Pelinovsky, T. Talipova, and C. Kharif. *Physica D: Nonlinear Phenomena*, 147(1-2):83–94, 2000.

[11] S. Popinet. *J. Comput. Phys.*, 190(2):572–600, 2003.

[12] P. Watts. PhD thesis, California Institute of Technology, 1997.